Wave analysis of intrinsic phenomena related to anisotropic poroelastic materials in multilayered systems

J. P. Parra Martinez [1,2*], **P. Göransson** [1], **O. Dazel** [2], **J. Cuenca** [1,3], **L. Jaouen**[4]
[1] ECO^2/MWL KTH Royal Institute of Technology,
Teknikringen 8, SE-10044, Stockholm, Sweden
LAUM - UMR CNRS 6613,

[2] LAUM - UMR CNRS 6613,
Avenue Olivier Messiaen, F-72085, Le Mans, France

[3] Siemens Industry Software
Interleuvenlaan 68, B-3001, Leuven, Belgium

[4] Matelys-Research Lab,
Bat. B, 7 Rue des Maraîchers, F69120 Vaulx-en-Velin, France

[*] e-mail: **jppm@kth.se**

Abstract
An analysis of intrinsic dynamic phenomena in anisotropic poroelastic media is presented, based on a plane wave formulation. The latter is derived from the Stroh formalism on the state variables governing the behaviour of such media. A particular interest is given to the compression-shear coupling related to the material alignment of the anisotropic poroelastic core. This coupling motion can be directly correlated to the material mechanical parameters and affects the response of the overall structure in specific frequency ranges. Furthermore, the effect of the anisotropic poroelastic material coordinate orientation on the the acoustic and elastical response of multilayered systems with such material cores is investigated under diffuse field excitation conditions (i.e. only a part the mechanics which doesnt include maximum stress at rupture). An insight into other effects of anisotropy is provided, such as the frequency shift of the fundamental resonance related to the core material alignment and the appearance of particular geometrical coincidences in the acoustic behaviour of the system.

1 Introduction

Poroelastic materials (PEMs) are widely used in different domains of physics for their low weight and high dissipative characteristics/properties [1–3]. Thus, physical models for the mechanical and acoustic behaviour of such materials have been developed for geophysical applications [4–6] and adapted to mechanical engineering applications [7]. Previously accepted as mechanically and acoustically isotropic, the development of recent characterisation techniques have shown that PEMs are inherently anisotropic [8–11] due to the manufacturing process.

In order to observe the influence of the anisotropy of PEMs in the acoustic behaviour of multilayered systems, a model was developed [12]. There, the authors found an important influence of the relative alignment of anisotropic PEM with respect to the system under normal and oblique incidence. Additionally, the phenomena responsible for such behaviour was found to be different with respect to a system with the closest isotropic equivalent.

In this paper, the authors investigate the influence of the relative alignment of PEMs in multilayered structures under diffuse field excitation and compare it to the case under a single plane wave excitation. Moreover, an analysis of the wave phenomena governing the behaviour of the system is presented.

2 On the modelling of the acoustic multilayered problem

2.1 Governing equations

The dynamic behaviour of any homogeneous linear physical medium, under harmonic excitation with circular frequency ω, can be modelled by a general system of first-order equations in a Cartesian coordinate system (xyz). It is assumed that the medium is a constituent of a multilayer system, infinite in the xy-plane with interfaces normal to the z-direction and that this system is excited by a plane wave with prescribed wavenumbers k_x, k_y. Partial differentiation with respect to coordinates x and y become algebraic operations such that the dynamic state of a homogeneous medium may be written as a system of linear equations,

$$\left(\mathbf{R} + \mathbf{A}_z \frac{\partial}{\partial z}\right) \mathbf{w}(z)\, e^{\jmath(\omega t - k_x x - k_y y)} = \mathbf{0}, \tag{1}$$

where

$$\mathbf{R} = \mathbf{A}_0 - \jmath k_x \mathbf{A}_x - \jmath k_y \mathbf{A}_y. \tag{2}$$

$\mathbf{w}(z)$ is a vector of physical field variables used in the modelling. The Biot model in the $\{\mathbf{u}^s, \mathbf{u}^t\}$ representation [13] is adopted, and adapted to the representation for anisotropic poroelasticity [14]. The governing equations under the form of Eq. (1) may be found in the literature [12].

In the following, the common spatial and time dependence $e^{\jmath(\omega t - k_x x - k_y y)}$ is omitted.

The introduction of the spatial dependence prescribed by the wavenumbers k_x, k_y introduces a linear dependence among the fields in $\mathbf{w}(z)$. Out of the field amplitudes in $\mathbf{w}(z)$, n are linearly independent. Thus, a partitioning of $\mathbf{w}(z)$ may be performed, as

$$\mathbf{w}(z) = \begin{Bmatrix} \mathbf{s}(z) \\ \mathbf{s}_0(z) \end{Bmatrix}, \tag{3}$$

where $\mathbf{s}(z)$ is a state vector of the system of length n.

The evolution of $\mathbf{s}(z)$ can be rewritten in the form of a state space representation [15],

$$\frac{\partial}{\partial z}\mathbf{s}(z) = -\boldsymbol{\alpha}\, \mathbf{s}(z), \tag{4}$$

where $\boldsymbol{\alpha}$ is referred to as the state matrix. An algorithm to calculate the state matrix for isotropic and fully anisotropic PEMs can be found in the literature. [12, 16].

2.2 Acoustic response

The transfer matrix $\mathbf{M}(z, z_0)$ between two points in the medium z_0 and z may be obtained by solving Eq. (4) for the state vector at these two points,

$$\mathbf{s}(z) = \mathbf{M}(z, z_0)\ \mathbf{s}(z_0), \tag{5}$$

with

$$\mathbf{M}(z, z_0) = \mathbf{e}^{-(z - z_0)\boldsymbol{\alpha}}, \tag{6}$$

where $\mathbf{e}^{[.]}$ is the matrix exponential operator. Thus, the acoustic response in the space of field variables of a multilayered system including anisotropic PEMs may be calculated by successively applying the transfer matrices of the corresponding layers,

$$\mathbf{s}(z_L) = \left\{ \prod_{l=L}^{1} \mathbf{M}_l \left(z_l, z_{l-1}\right) \right\} \mathbf{s}(z_0), \tag{7}$$

where z_l is the reference (incidence) point in layer $l = 1, \cdots, L$, z_L is the observation point in the last layer, L, and z_0 is the observation point in the first layer, $l = 1$.

2.3 Wave behaviour

By addressing the unsymmetric eigenvalue problem associated with the state matrix,

$$\boldsymbol{\alpha} = \boldsymbol{\Phi}\, \boldsymbol{\Gamma} \boldsymbol{\Phi}^{-1}. \tag{8}$$

where $\boldsymbol{\Phi}$ and $\boldsymbol{\Gamma}$ are respectively a matrix whose columns are the n eigenvectors and a diagonal matrix with the n nonzero eigenvalues, the solution of Eq. (1) in terms of the state vector $\mathbf{s}(z)$ may be expressed as a superposition of waves in the medium,

$$\mathbf{s}(z) = \boldsymbol{\Phi}\, \boldsymbol{\Lambda}(z)\, \mathbf{q}, \tag{9}$$

where $\mathbf{q}$ is a vector containing the contribution of the n waves in the layer, and $\boldsymbol{\Lambda}(z) = \mathbf{e}^{-\boldsymbol{\Gamma} z}$ describes the propagation in the layer. Thus, the acoustic behaviour in the eigenspace of a multilayered system including anisotropic PEMs may be calculated.

By specifying boundary conditions, material parameters and incident field on the multilayer system, both the wave field and the state variables are obtained.

2.4 Dynamic behaviour

Indicators such as the dissipated powers by elastical, thermal or visco-inertial effects, or the kinetic powers in the PEM, may be derived by integrating quadratic terms over d, the thickness of the medium. Thus, a time-averaged and space-integrated quadratic term $\mathcal{P}$ is expressed in terms of the wave properties and contributions as,

$$\mathcal{P} = \mathbf{q}^* \left[\int_0^d \boldsymbol{\Lambda}^*(z)\, \boldsymbol{\Phi}^*\, \boldsymbol{\Xi}\{\mathcal{P}\}\, \boldsymbol{\Phi}\, \boldsymbol{\Lambda}(z)\, \mathrm{d}z \right] \mathbf{q}, \tag{10}$$

The expression of the quadratic factor $\boldsymbol{\Xi}\{\mathcal{P}\}$ depends on the physical fields involved on the calculation of the indicator.

3 Application

The multilayered system corresponds to a sandwich panel composed of two 1mm aluminum face sheets and an 88mm anisotropic melamine foam.

The system is excited by a diffuse field incident on one of the face sheets, modelled as a superposition of plane waves with incidence ranging from 0 to 70 deg for the altitude angle, and from 0 to 360 deg for the azimuth angle. The angles are distributed according to Gauss-Legendre quadratures using 12 points for the azimut distribution, and 12 points for the altitude distribution, for which the convergence was found suitable. The opposing face sheet is coupled to a semi-infinite fluid where the radiated acoustic field is observed.

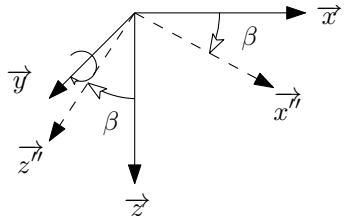

Figure 1: Rotations of the poroelastic material coordinate system with respect to the global coordinate system along the y axis.

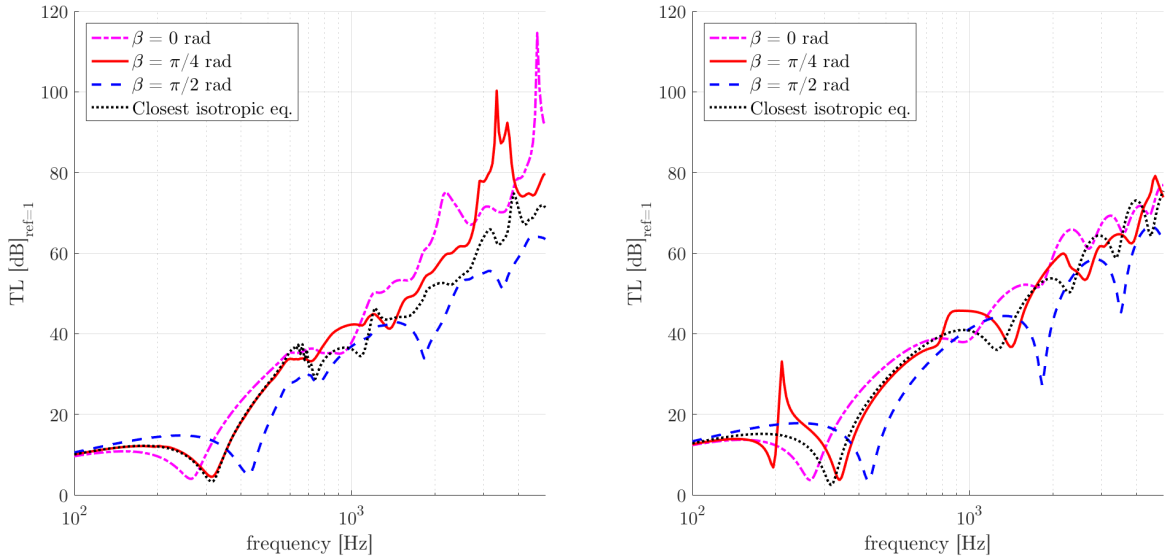

Figure 2: Transmission loss under 2(a) diffuse field, and 2(b) normal incidence [12].

The influence of the anisotropy of the PEM is observed by performing rotations on the materials coordinate system by an angle β around the y-axis, relatively to the global coordinate system, as depicted in Fig. 1.

Additionally, the response of the multilayered system with the anisotropic core is compared to that of an equivalent system composed of an isotropic poroelastic core. The material parameters of the core correspond to the closest isotropic equivalent material, as proposed by Norris [17].

The material parameters used in the following, as well as the results under normally incident excitation, may be found in the reference [12]. The dynamic behaviour will be discussed in three frequency ranges: low, $f \sim [100 - 500]$ Hz; mid, $f \sim [0.5 - 1]$ kHz; and high, $f \sim [1 - 5]$ kHz.

3.1 Acoustic response

Fig. 2 shows the acoustic response of the multilayered system in terms of Transmission Loss (TL) as a function of frequency for 3 different material orientations $\beta = [0; \pi/4; \pi/2]$ rad, under two different excitations: 2(a) diffuse field excitation, and 2(b) normally incident excitation.

As under normally incident excitation, the low frequency behaviour of the system under diffuse field excitation is characterised by a shift in the fundamental resonance as a function of β. However, the shear-compression coupling high amplitude resonance and antiresonance phenomena at $f \sim 200$ Hz observed under normal incidence does not appear under diffuse field. The high frequency response is characterised by

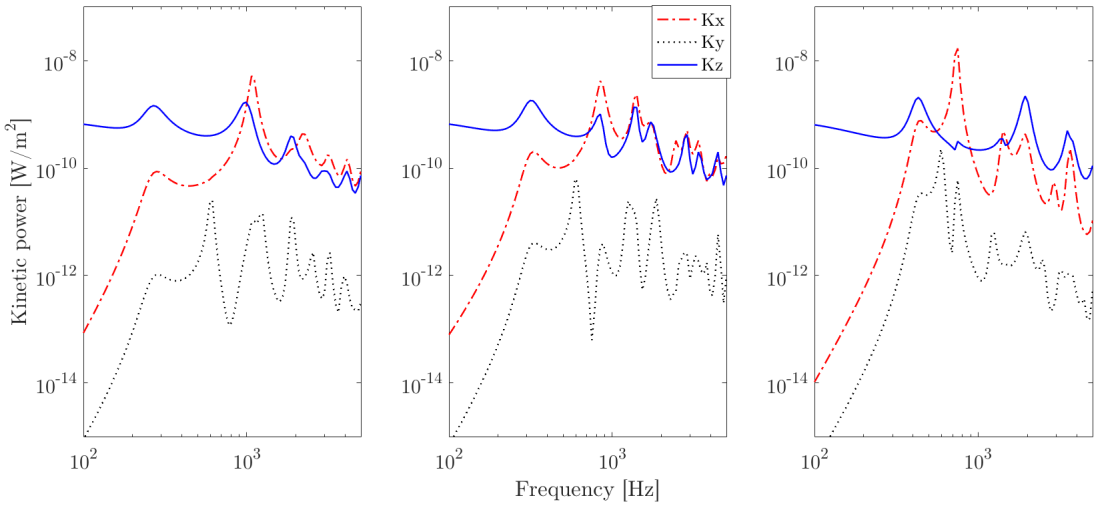

Figure 3: Kinetic power in the PEM as a function of the material alignment rotation under diffuse field excitation for (left) $\beta = 0$ rad, (centre) $\beta = \pi/4$ rad,and (right) $\beta = \pi/2$ rad.

resonant behaviour under both excitations, with particularly high amplitude anti-resonances appearing under diffuse field excitation.

3.2 Dynamic response

The total kinetic power in the PEM under diffuse field excitation can be observed in Fig. 3 for three different material alignments. The response of the system is overall governed by the kinetic power on the z-direction. The kinetic power on the y-direction has very little influence on the total kinetic power of the structure regardless of the material orientation of the core. Nonetheless, the high frequency response of the system if governed by the kinetic power on the x-direction, all the most for particular frequencies where the order of magnitude of K_x is considerably larger than the order of magnitude of K_z.

3.3 Mechanical behaviour

3.3.1 Fundamental resonance frequency shift

The frequency shift of the fundamental resonance of the multilayered system as a function of β may be seen in Fig. 4 under both normally incident and diffuse field excitations. In addition, therein may be observed the variation of the term $\sqrt{\hat{H}_{33}}$ as a function of β. This term is the square root of the stiffness coefficient that relates the compressional deformation rate ϵ^s_{zz} in the solid phase of the PEM with the compressional stress rate $\hat{\sigma}_{zz}$.

As it can be observed, the frequency shift of the fundamental resonance under diffuse field has a closer correlation with the variation of $\sqrt{\hat{H}_{33}}$ than the frequency shift under normal incidence.

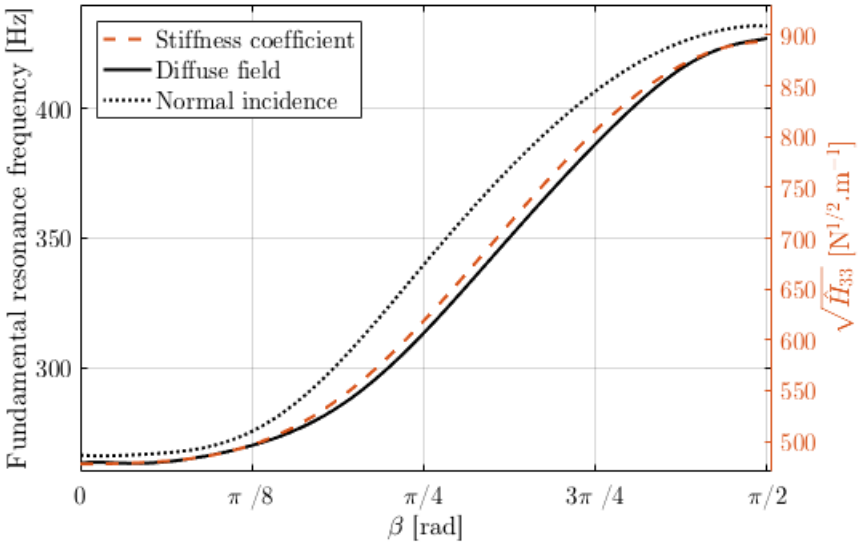

Figure 4: Fundamental resonance of the multilayered system under normally incident and diffuse field excitations, and stiffness coefficient $\sqrt{\hat{H}_{33}}$, as a function of the material alignment rotation

3.3.2 Relative deformation rate

Let $\left[\epsilon^s_{kl}(\omega)\right]_i$ (for $k,l = x,y,z$), be the strain in the solid phase of the PEM induced by the i-th wave ($i = 1,\ldots,n$) at the frequency ω. Thus, the relative deformation coefficient κ_{kl} may be defined as

$$\kappa_{kl}(\omega) = \frac{\sum_{i=1}^{n} \left|\left[\epsilon^s_{kl}(\omega)\right]_i\right|}{\sum_{k,l=x,y,z} \left\{\sum_{i=1}^{n} \left|\left[\epsilon^s_{kl}(\omega)\right]_i\right|\right\}}, \tag{11}$$

and translates the relative strains in the porous' solid phase on $\epsilon^s_{kl} = 1/2\left(\partial u^s_k/\partial l + \partial u^s_l/\partial k\right)$ relative to the total strain in the material.

Fig. 5 shows the relative deformation rate in the PEM core, as defined in Eq. (11), for three different material alignments under diffuse field excitation. It may be seen that the waves in the PEM induce a very small compression deformation on yy regardless of the material alignment, as well as negligible shear deformation on the xy-plane. Furthermore, the diffuse excitation induces waves predominantly polarised with a compression component on κ_{zz}, with a non-negligible shear deformation on the xz- and yz-planes. However, at $\beta = \pi/2$ rad, the material coordinate alignment induces waves predominantly polarised with a shear deformation component on κ_{xz}.

4 Discussion and conclusion

As previously observed [12], the material alignment of the anisotropic PEM core of a multilayered panel has a strong influence on the acoustic and mechanical response of the system under normal and oblique incident excitation. In the present work, it was observed that the behaviour under diffuse field excitation is noticeably affected by the material orientation both mechanically and acoustically, see Figs 2(a)-3.

The study has shed light onto particular phenomena inherent to anisotropic materials. Foremost, the frequency shift of the fundamental resonance of the system was found to be proportional to the compressional

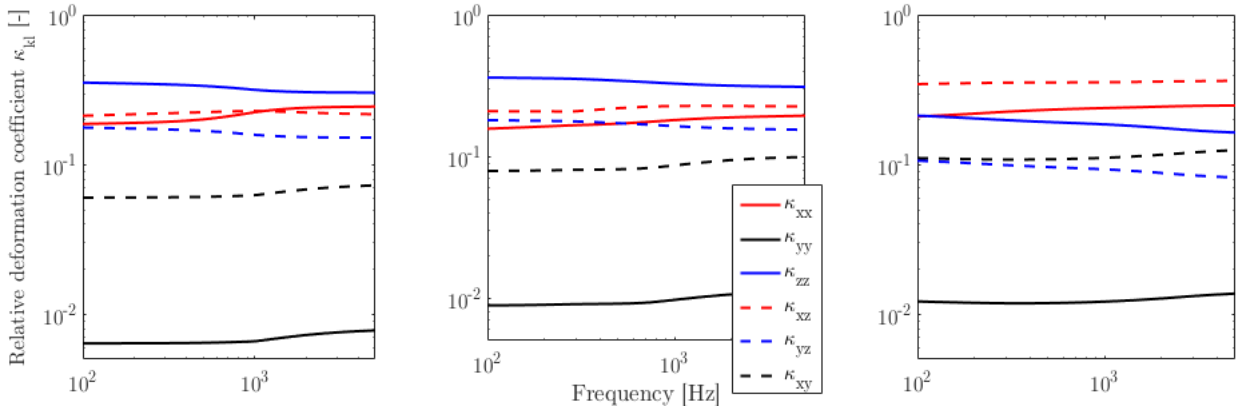

Figure 5: Relative deformation rate κ_{kl}, $(k, l = x, y, z)$, under diffuse field for 5(a) $\beta = 0$ rad, 5(b) $\beta = \pi/4$ rad, and 5(c) $\beta = \pi/2$ rad.

stress-strain rates coefficient $\sqrt{\hat{H}_{33}}$, as may be seen in Fig. 4. For an isotropic material, this coefficient is proportional to the phase velocity of the main compressional wave (in the form $c_\varphi = \sqrt{\text{stiffness/density}}$). Intuitively, at low frequencies the response of the material to a diffuse field would be less sensitive to its orientation and therefore its behaviour could be expected to be closer to an isotropic material. This is however not the case, as observed in Fig. 4. The observed effect of the diffuse field excitation is to reduce the low-frequency shear-compression coupling. Therefore the evolution of the first compressional resonance in the case of diffuse field incidence has a stronger correlation with $\sqrt{\hat{H}_{33}}$ than in the case of a plane wave excitation. This shows that the acoustic performance of the sandwich panel can be modified at all frequencies by changing the orientation of the PEM layer.

This behaviour allows to conclude that, for the herein tested materials, and regardless of the excitation under which the system is subjected to, the frequency of the fundamental resonance is not exclusively a function of the compressional stresses in the system. Thus, the fundamental resonance frequency can not be predicted by existing isotropic models, highlighting the need for more complete material models. Furthermore, it was observed that the dynamic profile, Fig. 3, in the PEM is governed by a motion in the z-direction at low frequency. This is in agreement with the relative deformation profile induced in the PEM, Fig. 5, which indicates that the motion corresponds to either a compressional deformation in the z-direction, or a shear deformation in the xz-plane.

The objective of this paper was to investigate the influence of the relative alignment of PEMs in multilayered structures under diffuse field and compare it to the case under a single plane wave excitation. The study found that there is indeed an influence of the material alignment regardless of the excitation. Finally, the work performed allowed to shed light onto different phenomena inherent to anisotropic poroelastic media, as well as to correlate mechanical parameters, wave polarisations and acoustic response of the overall structure.

References

[1] A. Färm, S. Boij, R. Glav, O. Dazel, *Absorption of sound at a surface exposed to flow and temperature gradients*, Applied Acoustics, Vol. 110, (2016), pp. 33–42.

[2] D. Wennberg, S. Stichel, *Multi-functional Design of a Composite High-Speed Train Body Structure*, Struct Multidisc Optim, Vol. 50, No. 3, (2014), pp. 475–488.

[3] M. F. Ashby, Y. J. M. Bréchet, *Designing hybrid materials*, Acta Materialia, Vol. 51, No. 19, (2003), pp. 5801–5821.

[4] M. A. Biot, *Theory of Propagation of Elastic Waves in a Fluid-Saturated Porous Solid. I. Low-Frequency Range*, Journal of the Acoustical Society of America, Vol. 28, No. 2, (1956), pp. 168–178.

[5] M. A. Biot, *Theory of Propagation of Elastic Waves in a Fluid-Saturated Porous Solid. II. Higher Frequency Range*, Journal of the Acoustical Society of America, Vol. 28, No. 2, (1956), pp. 179–191.

[6] M. A. Biot, *Generalized Theory of Acoustic Propagation in Porous Dissipative Media*, The Journal of the Acoustical Society of America, Vol. 34, No. 9A, (1962), pp. 1254.

[7] J. F. Allard, N. Atalla, *Propagation of Sound in Porous Media: Modelling Sound Absorbing Materials*, John Wiley & Sons, 2nd editio Ed. (2009).

[8] J. F. Allard, R. Bourdier, a. L'Esperance, *Anisotropy effect in glass wool on normal impedance in oblique incidence*, Journal of Sound and Vibration, Vol. 114, No. 2, (1987), pp. 233–238.

[9] R. Guastavino, *Elastic and acoustic characterisation of anisotropic porous materials*, Ph.D. thesis, KTH, School of Engineering Sciences (SCI), Aeronautical and Vehicle Engineering, Marcus Wallenberg Laboratory MWL, Stockholm, Sweden (2008).

[10] L. Jaouen, A. Renault, M. Deverge, *Elastic and damping characterizations of acoustical porous materials: Available experimental methods and applications to a melamine foam*, Applied Acoustics, Vol. 69, No. 12, (2008), pp. 1129–1140.

[11] C. Van der Kelen, J. Cuenca, P. Göransson, *A method for characterisation of the static elastic properties of the porous frame of orthotropic open-cell foams*, International Journal of Engineering Science, Vol. 86, No. 0, (2015), pp. 44–59.

[12] J. P. Parra Martinez, O. Dazel, P. Göransson, J. Cuenca, *Acoustic analysis of anisotropic poroelastic multilayered systems*, Journal of Applied Physics, Vol. 119, No. 8, (2016), pp. 084907.

[13] O. Dazel, B. Brouard, C. Depollier, S. Griffiths, *An alternative Biot's displacement formulation for porous materials.*, The Journal of the Acoustical Society of America, Vol. 121, No. 6, (2007), pp. 3509–3516.

[14] N.-E. Hörlin, P. Göransson, *Weak, anisotropic symmetric formulations of Biot's equations for vibro-acoustic modelling of porous elastic materials*, International Journal for Numerical Methods in Engineering, Vol. 84, No. 12, (2010), pp. 1519–1540.

[15] Q. Serra, M. N. Ichchou, J.-F. Deü, *On the Use of Transfer Approaches to Predict the Vibroacoustic Response of Poroelastic Media*, Journal of Computational Acoustics, (2015), pp. 1550020.

[16] O. Dazel, J.-P. Groby, B. Brouard, C. Potel, *A stable method to model the acoustic response of multilayered structures*, Journal of Applied Physics, Vol. 113, No. 8, (2013), pp. 083506.

[17] A. N. Norris, *The isotropic material closest to a given anisotropic material*, J. Mech. Mater. Struct., Vol. 1, No. 2, (2006), pp. 223–238.